TRACEABLE LOW ACTIVITY CONCENTRATION CALIBRATION OF RADON DETECTORS FOR CLIMATE CHANGE OBSERVATION NETWORKS

Röttger, Stefan[1] iD 0000-0002-4750-9563;

Annette Röttger[1] iD 0000-0001-6858-5795;

Florian Mertes[1,2] iD 0000-0003-0217-2845;

Scott Chambers[3] iD 0000-0002-2521-959X;

Alan Griffiths[3] iD 0000-0003-1135-1810;

Roger Curcoll[4] iD 0000-0002-8025-673X;

Claudia Grossi[4] iD 0000-0001-6678-4440;

[1] Physikalisch-Technische Bundesanstalt, Braunschweig, Germany.

[2] Bundesamt für Strahlenschutz, Neuherberg, Germany.

[3] Australian Nuclear Science and Technology Organisation (ANSTO), Sydney, Australia.

[4] Institut de Tècniques Energètiques (INTE) of the Universitat Politècnica de Catalunya (UPC), Barcelona, Spain.

TRACEABLE LOW ACTIVITY CONCENTRATION CALIBRATION OF RADON DETECTORS FOR CLIMATE CHANGE OBSERVATION NETWORKS

Stefan Röttger[a], Annette Röttger[a], Florian Mertes[a,d], Scott Chambers[b], Alan Griffiths[b], Roger Curcoll[c], Claudia Grossi[c]*

[a] Physikalisch-Technische Bundesanstalt, Braunschweig, Germany, Stefan.Roettger@ptb.de, Annette.Roettger@PTB.de
[b] ANSTO, Australia, Scott.Chambers@ANSTO.gov.au, Alan.Griffiths@ANSTO.gov.au
[c] Institute of Institute of Energy Technologies, Universitat Politècnica de Catalunya, Spain, Roger.Curcoll@upc.edu, Claudia.Grossi@upc.edu
[d] Bundesamt für Strahlenschutz, Germany, FMertes@bfs.de
* Corresponding author

Abstract – Radon gas is the largest source of public exposure to naturally occurring radioactivity, and concentration maps based on atmospheric measurements aid developers in complying with EU Safety Standard Regulations. But radon can also be used as a tracer to evaluate dispersal models important for supporting successful greenhouse gas (GHG) mitigation strategies. That is why reliable measurements of low-level radon activity concentrations, such as those found in the environment (< 20 Bq·m^{-3}), are important for both radiation protection and climate research. Despite the enormous changes in radon metrology that have occurred in recent years activity concentrations below 100 Bq·m^{-3} had not been subject to metrological research so far. This evokes new challenges which are the development of traceable methods and robust technology for measurements of environmental low-level radon activity concentrations and radon fluxes from the soil. Both are important to derive information on greenhouse gas fluxes in the environment and therefore are important for planning the reduction strategy.

In the framework of the EMPIR project 19ENV01 traceRadon [1], stable atmospheres with low-level activity concentrations of radon have been produced to enable calibration of radon detectors capable of measuring these environmental activity concentrations. The required traceability of the calibration at very low activity concentrations, was not possible in the past.

To achieve this goal, low activity sources of radium have been produced [2,3] with different methods and different characteristics. Sources down to few Bq of ^{226}Ra have been developed and characterized leading to uncertainties as low as 2 % (*k*=1), even in case of the lowest activity sources. Additionally, sources with medium and high activities were produced, with advanced production methods like ion implantation of mass separated ^{226}Ra in different target materials.

As an outcome, for the first-time traceable methods for measuring low-level atmospheric radon activity concentrations in the range of 1 Bq·m^{-3} to 50 Bq·m^{-3} with uncertainties below 5 % (*k*=1) are now available. To compare the performance of the sources in application, e.g., to establish a reference atmosphere, a calibration exercise with two highly sensitive, large volume, low radon activity concentration detectors of different design and principle was carried out at the PTB. The details of the calibration procedure of these unique prototypes of detectors are presented. The results of the
characterization of the detectors are discussed and as a conclusion new developments in the field of radon metrology are presented.

1. INTRODUCTION

The topic of radon metrology is not new: In fact, radon has been a challenge in radiation protection for centuries. But it developed a completely new guise in the field of environmental measurement networks for climate monitoring. As a noble gas, it is an ideal trace for estimating greenhouse gas fluxes. With its help, carbon dioxide or methane fluxes from the ground over a broadly distributed region [4] can be measured and used for climate modelling. Thus, the radioactive element radon turns out to be a stroke of luck for climate research: Metrology has successfully provided solutions to make use of radon in climate observation and to use the same data to better protect people against its harmful effect. Consequently, the results from 19ENV01 traceRadon gained worldwide attention: For calibration, intercomparisons [5], the development of new instrumentation and atmospheric models.

2. METHODS OF RADON CALIBRATIONS

2.1. Classification of calibration procedures

Traceability of activity concentration (Bq·m^{-3}) in the concept of the revised SI system means that the basic units second (s) and metre (m) are defined by fundamental constants and are realised by a National Metrology Institute (NMI). To realise the unit, the conventionally true value of the quantity to be measured has to be estimated, in this case the radon activity concentration. The following procedures for this have been established for application in so-called radon calibration chambers:

Procedure 1: A primary method based on a reference activity concentration realised by a primary radon gas standard

[6] and a calibration volume (both values are traceable to national standards). The result is a calibration factor for a measurement device (system under test) calibrated in such an atmosphere. Such a device can be addressed as a secondary standard afterwards.

Procedure 2: A secondary method based on calibration via a reference monitor enclosed in the same atmosphere as the system under test. This procedure is essentially based on procedure 1 as it implements a secondary standard (calibrated for instance by procedure 1) and uses it to determine the reference activity to determine a calibration factor of another device.

Procedure 3: A primary/secondary calibration in a constant atmosphere based on a radium emanation source. This method can be primary or secondary with respect to the components used. It is a long-term procedure (8 – 10 half-lives of ^{222}Rn), as radioactive equilibrium is needed. It can be operated in a closed system or in an open system.

Procedure 4: A primary calibration in a non-constant atmosphere based on a radium emanation source in a closed volume. The system under test needs high sensitivity to achieve small uncertainties. It is operated in a closed system implementing suitable instrumentation and a data-driven computation. As a result, it is no longer necessary to wait for equilibrium to be reached, as the procedure is based on data measured during the build-up phase [2, 7-9]. Furthermore, the data analysis yields complete information about the characteristics of the system under test, like background indication, calibration factor (k), or sensitivity ($k_c =1/k$) characteristic limits and linearity can be derived.

Procedure 5: A calibration by a primary single radon activity injection into a system under test: Pulse calibration.

2.2. Systems under test: ANSTO 200 L and ARMON v2

Two prototypes of new environmental radon monitors were tested at the PTB according to procedure 4: One monitor developed by the Australian Nuclear Science and Technology Organisation (ANSTO), the ANSTO 200 L and another one, the ARMON v2 from the Institute of Energy Technologies, Universitat Politècnica de Catalunya, Spain (INTE UPC).

The physical principle of operation of the ANSTO 200 L is that of a two-filter dual flow-loop radon detector [10]: Ambient aerosols, radon progeny (filter) and thoron (^{220}Rn) (delay volume) are removed from the sampled air, which then passes directly into a chamber as part of the first flow loop (the "external" or sampling flow loop). New radon progeny form in this chamber under controlled conditions. A second flow-loop (the "internal" flow loop) repeatedly draws this air through a second filter inside the chamber, which captures the newly formed progeny for counting. The α-decays of the short-lived ^{218}Po and ^{214}Po on this filter are counted using a zinc sulphide / photomultiplier tube (ZnS-PMT) assembly. The 30 min α-count rate relates to a radon activity concentration. This relation is given by calibration with a known source.

The physical principle of operation of the ARMON v2 is based on collection of positive ^{218}Po$^+$ cations [11], from the α-decay of ^{222}Rn within the detection volume, on the surface of a semiconductor detector. ^{218}Po$^+$ cations, generated within

a known volume, are found to be in the form of singly charged positive ions about 88 % of the time, while the neutral atoms occur the remaining 12 %. The ^{218}Po$^+$ is produced from the stripping of orbital electrons by the departing α-particle or by the recoil motion. When a high electric potential is applied to the internal surface of the detection volume and the detector itself is maintained at 0 V potential, an electrostatic field is generated inside the volume, causing the charged ^{218}Po$^+$ cations to be collected at the detector surface within short time. In the case of the ARMON v2, a Passivated Implanted Planar Silicon (PIPS) detector is used. A preamplifier and an amplifier are then used to amplify and shape the charge signal coming from the detector to a Gaussian function in order to be read by a multichannel analyser (MCA), which transforms it into counts for specific energy bins. The spectra generated can be analysed with commercial software. ARMON v2 makes use of MAESTRO (Multichannel Analyzer Emulation Software, from ORTEC).

2.3. Primary calibration in non-equilibrium

The SI traceability of a calibration with respect to ^{222}Rn activity concentration is realised by applying the procedure described by procedure number 4. The ^{226}Ra activity is provided through mass separated ion implanted sources as described in [7] which have been characterised according to their ^{222}Rn emanation applying Defined Solid Angle α-spectrometry (DSA) and γ-spectrometry using High Purity Germanium (HPGe) detectors [3]. The volume used for calibration is the climate chamber of PTB, formerly known as radon reference chamber with a free to air volume of $V_{chamber} = 21.224(17)$ m^3 in the case of the two described detectors placed inside the chamber volume.

Three different sources have been used in different combination, to achieve 5 different equilibrium activity concentrations. The ^{226}Ra emanation sources and their characteristic values are given in Table 1.

Table 1: The sources used for calibration with their unique names, activity of ^{226}Ra and emanation factor.

Source name	Activity Bq		Emanation
S2018_1121	1104	(5)	0.467(9)
S2018_1120	922	(4)	0.308(3)
S2018_1133	601.2(25)		0.273(4)

The temporal evolution of the produced ^{222}Rn activity concentrations with the measurement results of all the radon activity concentration detectors used for calibration or monitoring is shown in Figure 1. All values given are averaged values over 30 min of integration time.
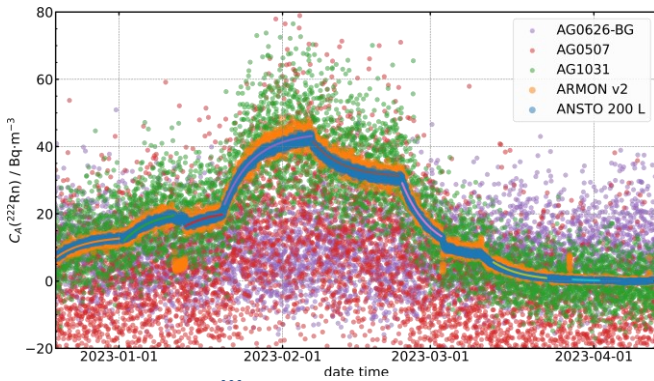
Figure 2: Calibrated ^{222}Rn activity concentration measurement results for different radon detectors. Three commercially available AlphaGUARD detectors of different age, in parallel with the two newly developed scientific outdoor air radon detectors (ANSTO 200 L, ARMON v2). AG0626 used as a background monitor in the lab room. All the others were placed in the calibration chamber measuring identical ^{222}Rn activity concentration.

The three commercial indoor air radon activity concentration detectors of type AlphaGUARD are marked with smaller dots and indicated as "AG". The scattering of the results, after calibration with values even below $C_A = 0$ Bq·m^{-3} prove that these detectors are not well suited for outdoor air activity concentration levels and time resolved measurements, simply because of their smaller active volume, which limits their counting statistics. AG0626 was used as a background and leakage monitor for the lab environment and was therefore placed in the climate controlled (100 % outdoor air, high air exchange rate) lab room.

The detailed results of this calibration exercise for the ARMON v2 detector as example are given in Figure 2 with the relative difference (residual) between the measured results and the produced ^{222}Rn activity concentration in air.

The coloured areas mark the different settings during the calibration for background and the different combinations of the sources explained in Table 1, used for this calibration.

Using this deviation between the primary derived calibration situation and the measurement results of the detectors used, the statistical distributions of the detectors are derived as a histogram and are shown in Figure 3.

The coloured areas in Figure 3 mark the 95 % coverage interval of the probability distribution for the results given by the respective detector. As a value in the respective colour the attributed statistical uncertainty for the expansion factor of $k = 2$ is given. The large difference of more than a factor of two between the two AlphaGURADs of the same type is explained with the age and the history of these detectors, which leads to different internal contamination of the detectors with ^{210}Po and therefore to different values of background subtraction. Larger values of subtracted background, especially for small count rates produces larger fluctuation in the difference. This already indicates that the determination of the background plays an important role in calibration of detectors for small activity concentration values with low desired uncertainty.
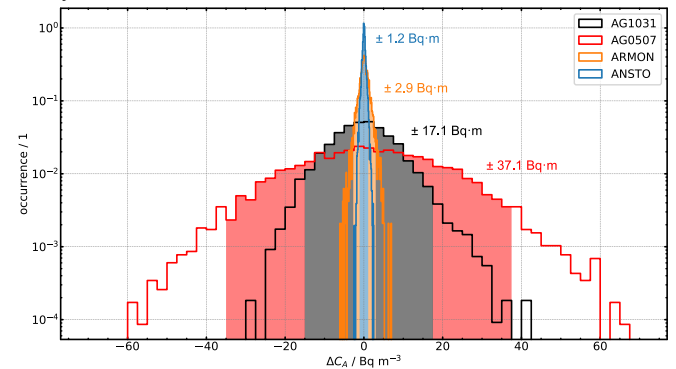

Figure 1: Statistical spread of the difference between measured values and the reference values derived from the sources as histogram in logarithmic presentation. The histograms are normalised to equal surface. The numbers given are the respective standard deviations of the histogram in Bq·m^{-3}. The coloured area is the 95 % coverage interval for the respective histogram

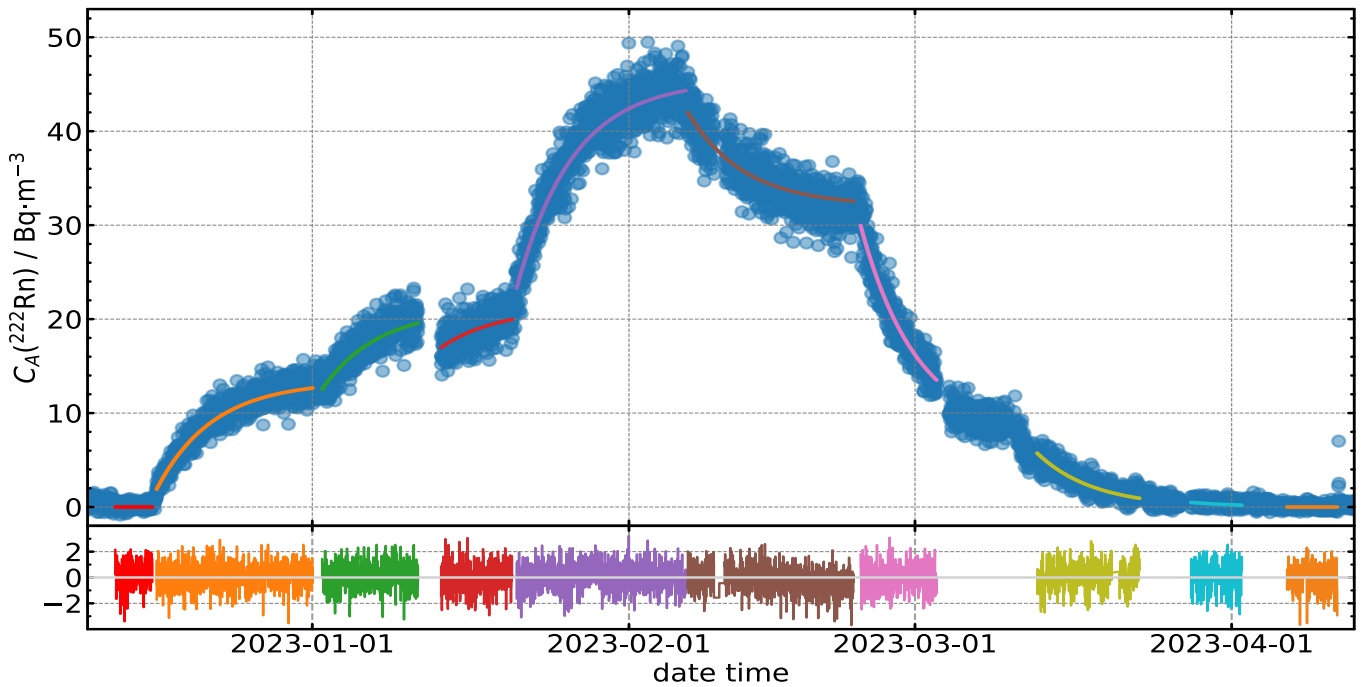Figure 3: $C_A(^{222}$Rn$)$ activity concentration measured in Bq·m^{-3} over time with the ARMON v2 compared with the ^{222}Rn activity concentration supplied by the reference sources in the traceable volume of the climate chamber.
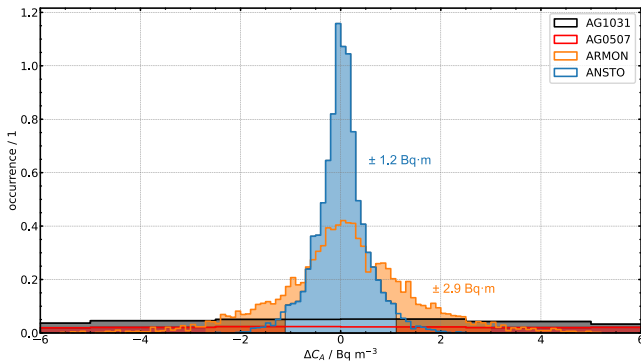
Figure 6: Statistical spread of the difference between measured values and the reference values derived from the sources as histogram in linear presentation. The histograms are normalised to equal surface. The numbers given are the respective standard deviations of the histogram in Bq·m⁻³. The coloured area is the 95 % coverage interval for the respective histogram.
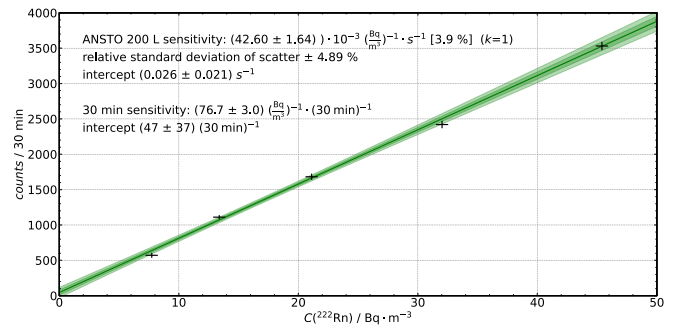

Figure 4: Results for the calibration factor of the ANSTO 200 L detector applying all sources and combinations measured, taking correlated and uncorrelated contributions of the source characterisation into account.
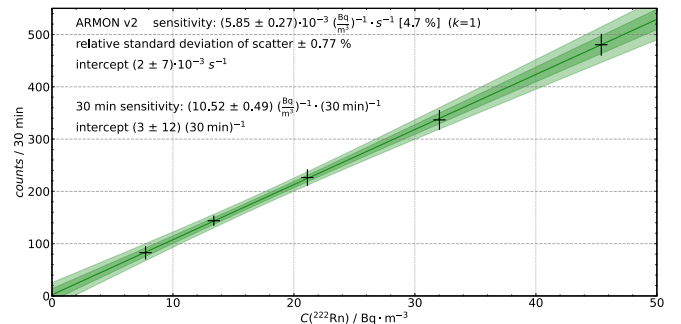

Figure 5: Results for the calibration factor of the ARMON v2 detector applying all sources and combinations measured, taking correlated and uncorrelated contributions of the source characterisation into account.

The values for the two scientific grade activity concentration detectors are given in more detail in Figure 4.

The width of the distribution in deviation of Bq·m⁻³ shows that the statistical fluctuations of the ANSTO 200 L is smaller than that of the ARMON v2, which can be explained by the active volume of these detectors. The internal flow loop of the ANSTO 200 L detector, that can be regarded as the active volume, has a volume of 200 L, whereas the electrostatic collection sphere of the ARMON v2, which is to be regarded as its active volume is only 20 L.

To determine a fully traceable calibration of the two detectors not only the statistical uncertainties of the measured count rates has to be taken into account but also the full uncertainty budgets of the calibration facility and sources. Since no secondary calibration standards (traceable devices) have been used, no transfer uncertainties must be considered. The characterisation of the sources includes several measurements which result in uncorrelated statistical uncertainties. The uncertainty of the primary α-activity measurement standard correlates with the uncertainty of all the sources. The determination of the sensitivity and the background of the detectors therefore includes correlated and uncorrelated uncertainty distributions for the detector measurements results as well as for the primary activity concentration production. This is taken into account applying an Orthogonal Distance Regression (ODR) in two steps for the uncorrelated uncertainty contributions and uncertainty propagation for the correlated uncertainty contributions. The resulting calibrations are summarised for the ANSTO 200 L in Figure 5 and the ARMON v2 in Figure 6. The dark green areas mark the uncertainty areas for $k = 1$, the light green areas for $k = 2$.

2.4. Calibration using pulsed activity

Instead of waiting for stable conditions and radioactive equilibrium, an alternative method is to use a defined, short pulse of ^{222}Rn activity and flush it through a detector. This, together with careful modelling, allows for much shorter calibration time and even a defined calibration volume is not needed. But the absolute activity is essential.

The evaluation of the results of the very recent pulse measurements show reasonable agreement with the sensitivity determined in Section 2.3.

This holds true for the ARMON v2 which again allows for spectral resolution as well as for the ANSTO 200 L which does not have the ability to distinguish between the different

progeny of ^{222}Rn within the detector output. The algorithm anyhow works as well with the sum of all progeny.

The results of the ARMON v2 measurements are shown in Figure 7: 3-dimensional representation of the time and energy (channel) resolved response of the ARMON v2 detector for a defined ^{222}Rn pulse applied at time 0 at the air inlet of the
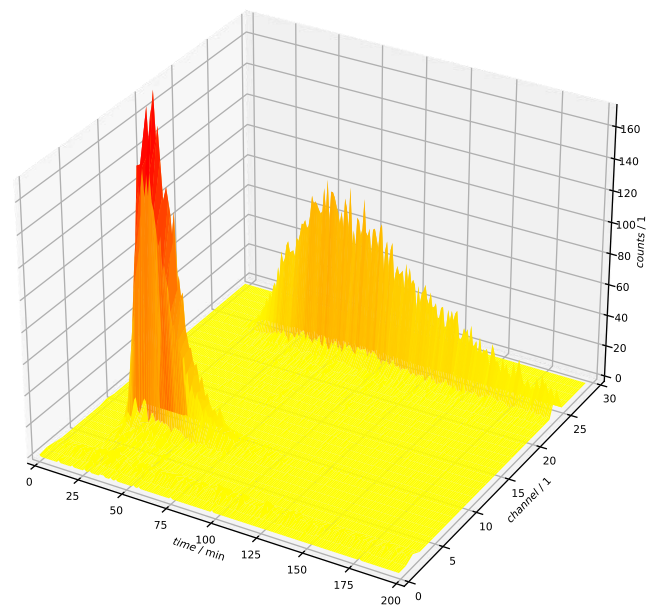

Figure 7: 3-dimensional representation of the time and energy (channel) resolved response of the ARMON v2 detector for a defined ^{222}Rn pulse applied at time 0 at the air inlet of the detector. At the lower channels (5-10) ^{218}Po represents the faster response of the detector and channel (20-30) the slower response of ^{214}Po is visible.
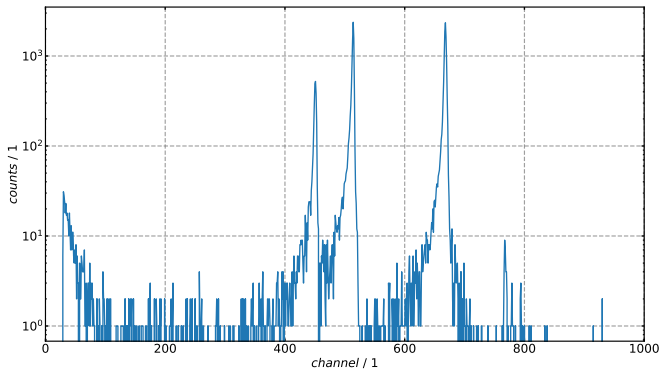
Figure 8: α-energy depended on distribution of events recorded with the ARMON v2 during the passage of a defined activity pulse of ^{222}Rn in logarithmic representation.

detector. At the lower channels (5-10) ^{218}Po represents the faster response of the detector and channel (20-30) the slower response of ^{214}Po is visible. Figure 7 is the 3-dimensional representation of the measured counts as a function of time and α-energy showing the whole information received during one pulse measurement.

Error! Reference source not found. is the projection of Figure 7 to the time axis showing the build-up, decay and flush out of the separate ^{222}Rn progeny.

While Figure 9 is the projection to the α-energy axis of the ARMON v2 and displays the energy resolution features of the detector showing the different progeny of ^{222}Rn that have been recorded during the pulse.

The detailed analysis of the data and the uncertainty of the pulse calibration is still in progress but seems to be in good agreement with the calibrations performed in section 2.3.

With this new type of calibration and the noticeably shorter time it takes to perform the calibration, a recalibration of detectors in field will become possible using ^{222}Rn free aged synthetic air, even at outdoor environmental activity concentration levels. Repeated calibration during measurement and applying ML techniques promises a calibration even with environmental air.

RESULTS AND DISCUSSION

The results of the calibration exercise as well as for both scientific detectors are remarkably good. Especially with respect to the fact that a fully SI traceable calibration of background and sensitivity has never before been carried out with all calibration points being below 50 Bq·m^{-3} and using a time resolution of 30 min. Remarkable as well is the achieved assigned uncertainty of below 5 % ($k = 1$) for the sensitivity of both detectors. The calibration uncertainty of the ANSTO 200 L detector is with 3.9 % a little bit smaller as for the AR-MON v2 whereas the standard deviation of the ARMON v2 measurements with regard to the produced activity concentrations, under this very constant laboratory conditions, is below 1 %. The background reading of the ARMON v2 is smaller than the ANSTO 200 L, which is due to its α-energy resolving capability and reduces its uncertainty even with a comparably smaller active volume.

3. CONCLUSIONS

One of the world's greatest challenges lies in combating climate change. Alongside this, the issue of radiological safety seemed less prominent for a long time, but the radioactive tracer "radon" combines both challenges. This brought together different scientific branches with a common need: new metrology for the determination of greenhouse gas fluxes and for the improvement of ambient dose monitoring networks in the environment.

Political decisions need valid data. Implementing expensive measures, whether in climate protection or radiation protection, always means the need to make the success of these measures measurable. Can metrology make its contribution here?

The consortium of the traceRadon project has taken up this challenge by looking for suitable metrics that could enable an assessment. This brought the radioactive noble gas radon into focus: Making measurable what was not measurable before, providing trustworthy data where there was no comparability before and thus paving the way for new approaches like the Radon Tracer Method (RTM) is a promising way how metrology can contribute to combat climate change. The traceRadon project showed what is possible when competences are brought together:

- new SI traceability chains for measurement quantities used in climate observation and radiation protection were developed,
- new customer calibration services were provided,
- new types of devices were made available,
- a standard protocol for the application of the Radon Tracer Method (RTM) to enable retrieval of greenhouse gas fluxes at atmospheric climate gas monitoring stations and to use radon flux data for the identification of Radon Priority Areas (RPA) was provided,
- Radon flux models and inventories have been validated,
- new traceable measurements of radon activity concentration and radon flux were supported by dosimetric and spectrometric data from the radiological early warning networks in Europe,
- as a further outcome easy to use dynamic radon and radon flux maps for climate change research and radiation protection in line with Council Directive 2013/59/EURATOM, including their use to identify RPA and radon wash-out peaks were provided.

But there is still some work to do for radiation protection: The growth of buildings in large cities and the fact that their air conditioning entails high energy costs, provides new challenges: Efficient insulation of the building and low air exchange rates will be desirable. However, strong insulation and low air exchange rate can lead to high levels of radon activity concentration. Therefore, the European Metrology Network for Radiation Protection (EMN RP) [12] identified this need as a top priority and the European Partnership on Metrology (EPM) provided funding for it with the project 23IND07 RadonNET within its 2023 industry call.

On the other hand, the Radon Tracer Method (RTM) established as a efficient tool for Green House Gas (GHG) estimates and climate modelling. From this the need for more SI traceable measurements with smaller uncertainties arose. And

led to the funding of a EURATOM project under FP9 (Horizon Europe) with the name "Nuclear observations to improve Climate research and GHG emission estimates" (NuClim), starting in 2024 and aiming to provide an accurate and time-varying baseline reference level for European GHG concentrations based on nuclear observations. The strategy to achieve this will make use of atmospheric radon concentration measurements at oceanic remote sites to identify baseline conditions, representative of hemispheric background values, which is essential for the improvement of the characterisation of the seasonality and inter-annual behaviours of radon concentrations in the marine boundary layer of the North Atlantic Ocean to assist the evaluation of transport and convective mixing schemes of global climate and chemical transport models. As well as to reduce the uncertainty on long-term trends in mid-latitude Northern Hemisphere baseline concentrations of selected GHGs to help reduce uncertainties in global climate change projections.

REFERENCES

[1] A. Röttger *et al: New metrology for radon at the environmental level, in Meas. Sci. Technol.* 32, 124008, 2021, DOI: https://doi.org/10.1088/1361-6501/ac298d

[2] S. Röttger et al.: **Evolution of traceable radon emanation sources from MBq to few Bq**, in Applied Radiation and Isotopes, Volume 196, 110726, 2023, DOI: https://doi.org/10.1016/j.apradiso.2023.110726

[3] F. Mertes et. al.: **Development of 222Rn emanation sources with integrated quasi 2π active monitoring**, in Int. J. Environ. Res. Public Health 2022, 19, 840, https://doi.org/10.3390/ijerph19020840

[4] I. Levin et al.: **Verification of German methane emission inventories and their recent changes based on atmospheric observations**, in J. Geophys. Res., 104, D3, 3447 – 3456, 1999. DOI: https://doi.org/10.1029/1998JD100064

[5] C Grossi et al.: **Characterizing the automatic radon flux transfer standard system Autoflux: laboratory calibration and field experiments**, in Atmos. Meas. Tech., 16, 2655–2672, 2023, https://doi.org/10.5194/amt-16-2655-2023

[6] J. L. Picolo: **Absolute measurement of radon 222 activity**, in Nuclear Instruments and Methods in Physics Research Section A, Volume 369, Issues 2–3, 1996, Pages 452-457, ISSN 0168-9002, DOI: https://doi.org/10.1016/S0168-9002(96)80029-5

[7] F. Mertes, et. al.: **Ion implantation of 226Ra for a primary 222Rn emanation standard**, in Applied Radiation and Isotopes, Volume 181, March 2022, 110093, DOI: https://doi.org/10.1016/j.apradiso.2021.110093

[8] S. Röttger, et al: **Radon metrology for use in climate change observation and radiation protection at the environmental level**, in Adv. Geosci., 57, 37–47, 2022, DOI: https://doi.org/10.5194/adgeo-57-37-2022

[9] A. Röttger, et al.: **Metrology infrastructure for radon metrology at the environmental level**, in Acta IMEKO, Vol. 12, No.2 (2023), DOI: https://acta.imeko.org/index.php/acta-imeko/article/view/1440

[10] S. Chambers, et al.: **Portable two-filter dual-flow-loop 222Rn detector: stand-alone monitor and calibration transfer device**, in Adv. Geosci., 57, 63–80, 2022, DOI: https://doi.org/10.5194/adgeo-57-63-2022

[11] R. Curcoll, et al.: **Full characterization and calibration of a transfer standard monitor for atmospheric radon and thoron measurements,** in EGUsphere, 2023, Preprint DOI: https://doi.org/10.5194/egusphere-2023-2680

[12] European Metrology Network for Radiation Protection Website: https://www.euramet.org/european-metrology-networks/radiation-protection/about-us (last accessed 2024-04-22)